Modelling and Simulation in Materials Science and Engineering

PAPER

Characterization of structure evolution of Ti–O clusters in molten iron

To cite this article: Liang He *et al* 2021 *Modelling Simul. Mater. Sci. Eng.* **29** 075006

IOP Publishing Modelling and Simulation in Materials Science and Engineering
Modelling Simul. Mater. Sci. Eng. **29** (2021) 075006 (13pp) https://doi.org/10.1088/1361-651X/ac1f86

Characterization of structure evolution of Ti–O clusters in molten iron

Liang He[1,2], Huigai Li[1,2,*], Minghao Liang[1,2], Wei Zhang[3], Ke Han[4] and Qijie Zhai[1]

[1] Center for Advanced Solidification Technology (CAST), School of Materials Science and Engineering, Shanghai University, Shanghai 200444, People's Republic of China
[2] State Key Laboratory of Advanced Special Steel & Shanghai Key Laboratory of Advanced Ferrometallurgy & School of Materials Science and Engineering, Shanghai University, Shanghai 200444, People's Republic of China
[3] Shanghai Institute of Applied Physics, Chinese Academy of Sciences (CAS), Shanghai, 201800, People's Republic of China
[4] National High Magnetic Field Laboratory, Florida State University, Tallahassee, FL 32310, United States of America

E-mail: lihuigai@i.shu.edu.cn

Received 24 May 2021, revised 26 July 2021
Accepted for publication 19 August 2021
Published 2 September 2021

Abstract

The interaction of Ti–O clusters with one another and with the surrounding steel melt results in changes in size and shape, which affect strength and hardness in the finished steel. We used MD simulation with two parameters that, together, describe the structure evolution of Ti–O clusters. These are: (1) the radius of pair gyration $\overline{R}_{g,p}$, which reflects the degree of the compactness of the cluster, and (2) the radial distribution function, which identifies the type of titanium oxide. The $\overline{R}_{g,p}$ value, which is inversely related to compactness, increases with the growth of clusters, then decreases abruptly when transformation occurs. Once the clusters form a particular TiO_x, the $\overline{R}_{g,p}$ value remains stable until next transformation. The growth of Ti–O clusters in molten iron is divided into three stages: unstable clusters → amorphous TiO structure → amorphous Ti_3O_5 structure. The mean critical size for the formation of amorphous TiO structure is about 7.0 Å × 9.6 Å × 21.6 Å. The critical size for the transformation of amorphous Ti_3O_5 structure is about 8.4 Å × 11.0 Å × 36.0 Å.

Keywords: molecular dynamics, Ti–O clusters, structure evolution, critical size

(Some figures may appear in colour only in the online journal)

*Author to whom any correspondence should be addressed.

1. Introduction

Strength and toughness in low-carbon steels can be enhanced by controlling the number and distribution of small dispersive titanium oxide inclusions that develop in molten steel when Ti and O atoms form clusters that then nucleate into oxides [1]. In a previous study, we tracked the evolution of simulated Ti–O clusters and found that they maintained a Ti:O ratio of 1:1 from the outset. As each O atom was attracted into a cluster, a Ti atom was also attracted, keeping the ratio at 1:1. Meanwhile, growing clusters collided with one another and formed larger clusters, and small-scale ($n \leqslant 12$) cluster structure had been studied [2, 3]. In this paper, the structure of larger-scale ($n \leqslant 346$) clusters will be studied and we will use a new parameter to study the structural changes of clusters during growth, which include (1) studying the formation and evolution process of Ti–O cluster's structure, (2) predicting the structure of TiO_x oxides after transformation and which cluster will change, and (3) describing the influence of the surrounding melt on the shape of the clusters.

Gibbs first developed classical nucleation theory (CNA), which believed that the transition from long distance disordered liquid to ordered solid was a one-step process [4]. Mahata *et al* calculated the critical nucleation size of Al by molecular dynamics (MD) to be 2.6 nm [5]. In recent years, several experimental studies provide evidence that the crystallization of ionic materials from aqueous solution proceeds through a transient amorphous phase but not one-step nucleation of a crystalline polymorph [6, 7]. Gebauer *et al* found that it will generate an amorphous calcium carbonate phase before the formation of any of crystalline polymorphs [8]. Chakraborty *et al* simulated the nucleation process of NaCl using MD and found that it experienced a two-step process [9]. To make clear if the nucleation of TiO_x inclusions is also a two-step process, we studied the formation and evolution process of Ti–O clusters in molten iron.

To identify the structure of clusters, we reviewed two commonly used methods from the literature: common neighbor analysis (CNA) [10] and bond angle analysis [11]. Mahata *et al*, for example, used CNA to simulate nucleation in Al [5]. This method is currently appropriate for single-element crystal structures, such as fcc, bcc, hcp, ISO, but not for multiple-element systems like TiO_x. Liu *et al* used bond angle analysis to simulate the nucleation process of NaCl clusters, a multi-element system [12]. This method depends on the comparison between simulated clusters and known crystal structure, giving close attention to coordination number, bond distance, and bond angle. This method introduces too much complexity, however, for use with multi-structured materials like TiO_x, which has five known crystal structures. To determine the exact structure of a simulated cluster, researchers would have to make hundreds of comparisons. We sought new parameters to identify the structural transformation of our Ti–O clusters and derived a parameter, which we called the radius of pair gyration, $\overline{R}_{g,p}$, to characterize the compactness of the clusters. It was derived from gyration radius (R_g). Ding found that the fluctuation of R_g can explain the stability of protein in the process of dynamics, and the value of R_g can explain the compactness of protein [13]. The R_g declined while the compactness of the system increased. When R_g reached the minimum value, the skeleton structure was more compact and reached a better stability.

This study explores the structure evolution of TiO_x inclusions with respect to changes in oxide type during growth, taking into consideration changes in cluster shape that would have resulted from the molten iron environment and not from the growth process itself.

2. Method

2.1. Settings

In this study, all simulations were carried out using the LAMMPS MD simulation program [14]. In order to counteract the influence of boundaries, we selected the periodic boundary condition in the program. We set the integration time step (the 'simulation moment') for 1 fs, the default value for metal systems. The formula for the Fe–Ti–O potential (the interaction between Fe, Ti, and O atoms) was introduced in detail in a previous study [2]. We set the size of our simulation box at 59.36 Å × 59.36 Å × 59.36 Å. Using PACKMOL, we randomly put in 16 200 atoms (15 800 of Fe, 200 of Ti, and 200 of O). Using the isothermal-isobaric (NPT) ensemble available in LAMMPS, we set the pressure at one atmosphere and the temperature at 2122 K, the setting smelting temperature of iron calculated with our potential; these settings are the same as those in our previous study [2]. In order to ignore the collision process and explore the final stable structure of large-size Ti–O cluster in molten iron, we constructed a Ti–O cluster with 4335 atoms by MS (Material Studio), which was placed in molten iron for 50 ns. The specific process is as follows: put a Ti–O cluster of 4335 atoms in the center of a cube box, and then randomly put 80 000 Fe atoms into the box to fill the box. Under the NPT ensemble, the Ti–O clusters were fixed first, the Fe matrix was melted to present a liquid structure, and then the bondage of the Ti–O clusters was released. Output the system energy at all times till the system energy reached an equilibrium value.

2.2. Simulation process

Ti–O clusters form in molten iron. The simulation process was divided into two stages. In the first stage, Ti and O atoms were fixed at 2122 K for 5 ns to ensure the complete melting of Fe. In the second stage, Ti and O atoms were loosened to simulate the growth process of Ti–O clusters in molted iron. At the beginning of the simulation ($t < 25$ ns), Ti and O atoms moved rapidly and formed clusters. The clusters and atoms then collided with one another, grew, and evolved in structure in molten iron. As time went on (25–50 ns), the system became stabilized. The distance between Ti and O atoms in clusters was counted at time of 50 ns. Results showed that the bond length of Ti–O was between 2.02 Å and 2.2 Å (figure 1). This length is comparable to that of the bonds in Ti_2O_3 (2.084 Å), $TiO_{2\text{-anatase}}$ (1.949 Å), and $TiO_{2\text{-rulite}}$ (1.96 Å), obtained by first-principles simulation [3]. It is also comparable to the length of bonds detected by XRD in $TiO_{2\text{-anatase}}$ (1.96 Å) [15].

The LAMMPS program allowed us to check the coordinates of Ti–O clusters every 2 ps. We used OVITO software to visualize possible cluster shapes based on those coordinates. We tracked structural changes in Ti–O clusters during the growing process.

2.3. Calculation process and analysis method

We used the mass-radius formula to calculate R_g, i.e. the distance from atom center to molecular center [16], which is related not only to the compactness of the calculated objects but also to their morphology and their atom numbers [17]:

$$\overline{x} = \sum_{i=1}^{n} \frac{x_i m_i}{m} \overline{y} = \sum_{i=1}^{n} \frac{x_i m_i}{m} \overline{z} = \sum_{i=1}^{n} \frac{x_i m_i}{m} \tag{1}$$

$$R_g = \sqrt{\frac{\sum_{i=1}^{n} (x_i - \overline{x})^2 + (y_i - \overline{y})^2 + (z_i - \overline{z})^2}{n}}, \tag{2}$$

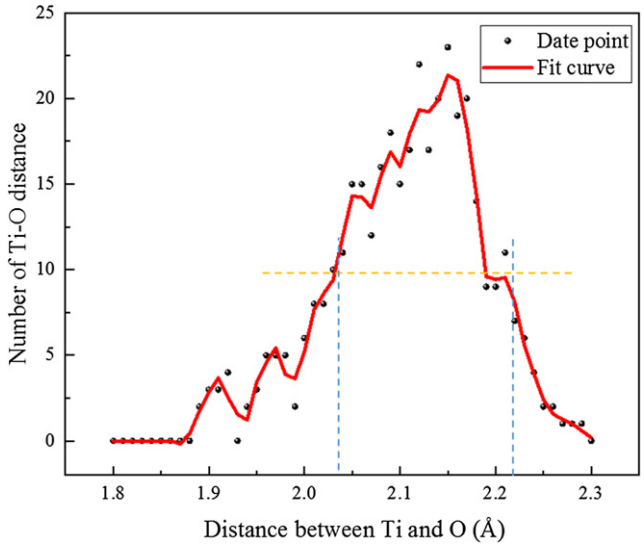

Figure 1. Ti–O distance distribution during the period of stability. The dotted blue lines delimit the range of Ti–O distance for the top 50% of clusters, those above the median (dotted yellow line).

where R_g is the radius of gyration; x_i, y_i, z_i are the coordinates for atom i; m_i is the mass for atom i; m is molecular mass; $\overline{x}, \overline{y}, \overline{z}$ are molecular coordinates; and n is the number of atoms.

To predict the structure evolution during the growth of our Ti–O clusters, we used R_g to present only the compactness of the structure but not their morphology and their atom numbers. The R_g value is defined here as the average distance (radius) from the center of the mass of an entire cluster to the center of a given TiO pair. From the R_g can be derived the $R_{g,p}$, which is defined as the radius of the space occupied by a given TiO pair after excluding the effect of the atom number of the cluster. This value is derived as follows [18]:

$$R_{g,p} = \frac{R_g}{\sqrt[3]{n/2}}, \tag{3}$$

where n is the number of atoms. p is the TiO pair (Ti:O is close to 1:1 in our simulated clusters), TiO pair is considered as the basic unit in our calculation.

In addition to excluding the effect of the atom number of a cluster, we needed also to exclude the effect of morphology. To do so, we relied on a widely used formula to calculate sphericity [19]:

$$\Psi = \frac{S_1}{S_2}, \tag{4}$$

where Ψ is the sphericity, S_1 is the surface area of a perfect ball with the same volume as the cluster, and S_2 is the actual surface area of the cluster.

Once we calculated sphericity, we could then derive the $\overline{R}_{g,p}$, which is the radius of the TiO pair after excluding the effect of both the atom number and the morphology of the cluster. This value is derived as follows:

$$\overline{R}_{g,p} = \Psi \cdot R_{g,p}. \tag{5}$$

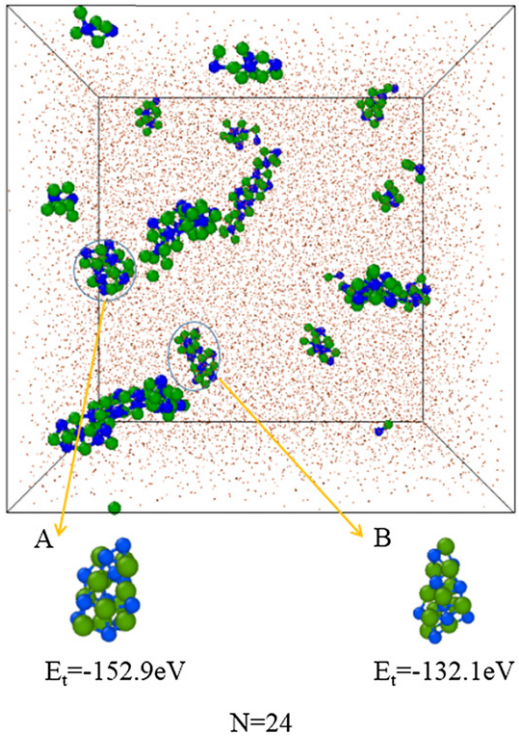

Figure 2. Morphology of Ti–O clusters at simulation time of 4 ns, Ti in green, O in blue, and Fe in brown. Enlargements of two 24-atom clusters (A and B) from the same simulation moment but with different morphologies are shown below the box. (The Fe atoms are here reduced by 10× in order to emphasize Ti and O.)

In our simulation, there were a great many clusters with low numbers of atoms, but only a few with high numbers. We selected 23 sets of ten clusters each to represent those containing from 4 to 46 atoms, and from the remaining clusters, we assembled sets of various sizes to represent atom numbers from 48 on. For each set, we calculated the average R_g, from which we derived the $\overline{R}_{g,p}$, a value that corresponds only to compactness, excluding the effect of morphology or atom numbers. This value identifies the exact point of structure transition in Ti–O clusters.

3. Results and discussion

3.1. Structural changes during cluster growth

By tracing the coordinates of Ti and O atoms in a simulated Fe–Ti–O system, we studied the structure changes that accompany cluster growth. We isolated Ti–O clusters at each simulation moment. Sometimes, multiple Ti–O clusters with the same atom number have different morphologies at the same simulation moment (see figure 2). One of these similar clusters is likely to have the lowest total energy (E_t) and thus be more stable at that moment than the others [20]. The calculation of E_t includes both the kinetic energy and the potential energy of each atom in a cluster [21]. Thus, calculation of E_t at each moment allowed us to predict structure

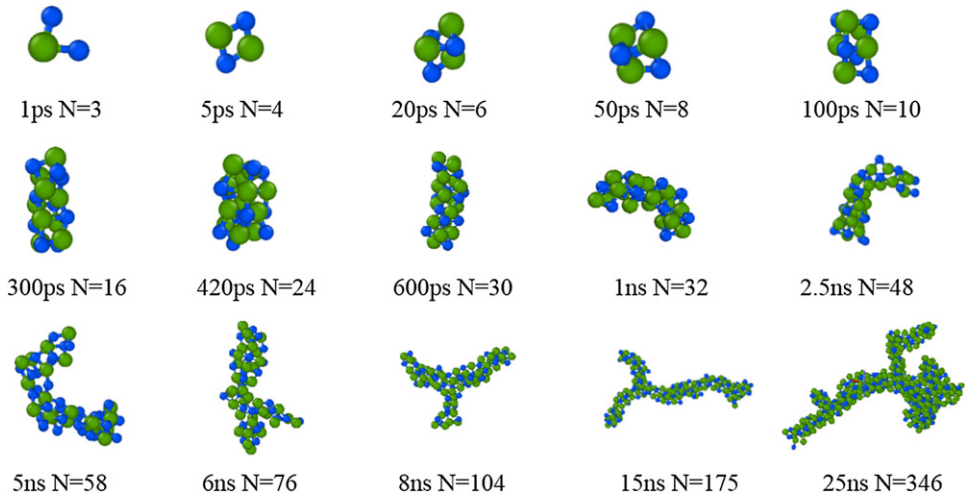

Figure 3. Morphology changes in Ti–O clusters of lowest energy with atomic numbers varying. (Ti in green, O in blue.)

evolution in the growing process by identifying the most stable clusters, which are more likely to survive and grow than some of the others of the same atom number.

We used the most stable cluster of each atom number at each simulation moment to trace morphology changes during the growth process of Ti–O clusters (figure 3). When the atom number (N) is 4 or less, the most stable structure is planar. When N is from 6 to 30, the most stable structure is cuboid. When N is from 32 to 68, the most stable structures are worm-like shapes. When N is larger than 72, the worm-like shapes also have dendritic branches.

3.2. Ti–O cluster's structure transition

When a Ti–O cluster form a particular structure, its compactness will keep constant. The $\overline{R}_{g,p}$ allowed us to predict the precise moment of structure transformation; we measured the critical size of the cluster at that moment. By comparing $\overline{R}_{g,p}$ values of the clusters in stage and stage with those of known crystal structures, we could preliminary speculate that one type of oxide structure formed in stage and it transformed into another type in stage .

When the number of atoms is 68 or less (stage), $\overline{R}_{g,p}$ increases with the increase of the number of atoms in the cluster, which means that the cluster becomes looser (figure 4). We performed RDF (Ti–O) computation for two randomly selected Ti–O clusters, one with 36 atoms and the other with 68, and we found two peaks: the first at 2–2.5 Å and the second at 4–6 Å (figure 7). The presence of these peaks indicates disordered structure [22, 23]. Lundqvist *et al* studied a series of Ti–O cluster models using the first principle method and found that Ti–O cluster structure is not periodic when atom number is less than 68 [24]. We confirmed that Ti–O clusters are unstable when the atom number is less than 68.

The loosening of a given Ti–O cluster during its growing process provides sufficient space for surface atoms to move out of or for external atoms to move into the cluster. In this way, the cluster can adjust its shape and prepare for structural transformation in the later stage. In our previous study, we observed Ti and O atoms moving from the melt onto the surface of a cluster or from the surface of the cluster into the melt [2]. We calculated the distances between Ti and O atoms in a series of clusters whose atom numbers are 48, 58 and 68. These distances were

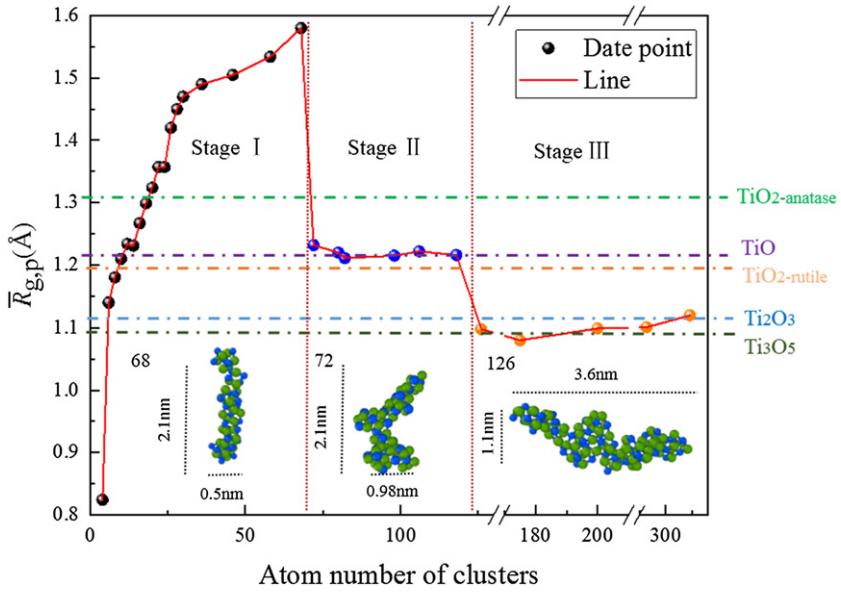

Figure 4. The relationship between $\overline{R}_{g,p}$ and the atom number of clusters. $\overline{R}_{g,p}$ increases in stage and keeps constant in both stage and stage . Base on $\overline{R}_{g,p}$, the structure of the oxide in stage is similar to TiO; the structure of the oxide in stage is resembled either Ti_2O_3 or Ti_3O_5.

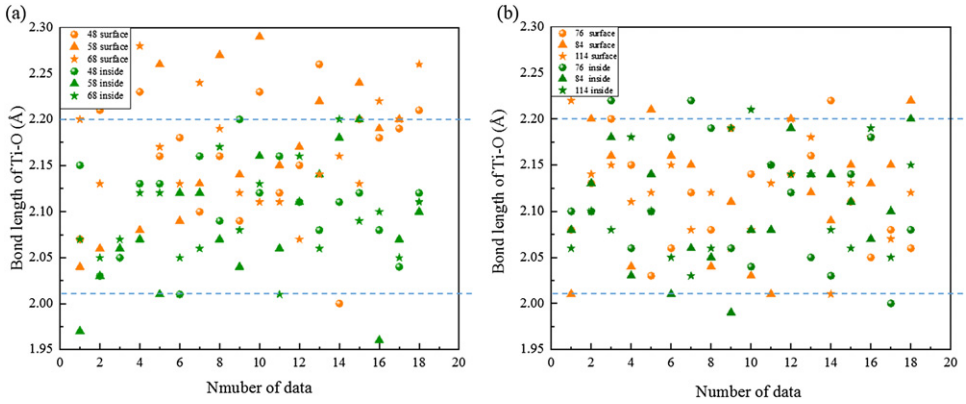

Figure 5. Distance between Ti and O inside and on the surfaces of clusters both in unstable stage (a) and in stable stages (b), whose atom numbers are 48, 58, 68, 76, 84 114. The dotted blue lines represent the Ti–O bond length between 2.02 Å and 2.2 Å.

smaller inside clusters than on cluster surfaces. Inside clusters, almost all distances fell within the range of the Ti–O bond length, but on cluster surfaces nearly half were greater (figure 5(a)). We deduced that the greater distances between Ti and O atoms on cluster surfaces makes them less stable and more active than Ti and O atoms inside clusters. Thus, surface atoms are more likely to transfer onto other clusters or into the melt, contributing to shape adjustments that can prepare the cluster to form a stable structure.

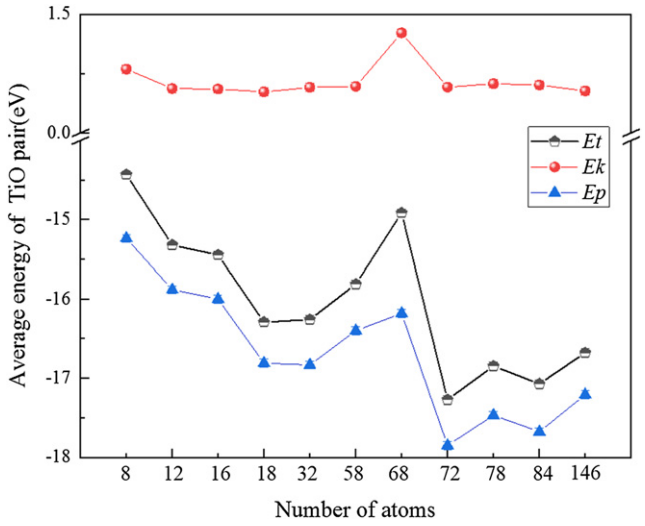

Figure 6. The relationship between energy of every TiO pair and the atom number of clusters. E_t is total energy, E_p potential energy, E_k kinetic energy.

The $\overline{R}_{g,p}$ value decreases suddenly when the atom number increases from 68 to 72. When the atom number is between 72 and 120 (stage), the $\overline{R}_{g,p}$ value remains stable at about 1.2 Å, which indicates that the arrangement inside the cluster has taken the form of a particular titanium oxide. When $N = 72$, the transition from unstable to stable structure occurs, and the continuous loosening of the original atom arrangement transforms suddenly into a compact, stable form. We concluded that Ti–O structure is formed when the atom number reaches an average of 74 and the critical size reaches an average of 7.0 Å × 9.6 Å × 21.6 Å. To confirm the consistency of these values, we repeated our simulation of Ti–O cluster growth numerous times.

We confirmed the formation of Ti–O structure in stage in aspects of both Ti–O bond length and energy of TiO pair. Using similar method in stage , we calculated the distance between Ti and O atoms in clusters with atom numbers of 76, 84 and 114 (figure 5(b)). Results showed that the Ti–O bond length of surface atoms is in the same range with that of inner atoms, which indicates the clusters' structure is stable in stage . The average energy of TiO pairs in clusters drops sharply when the atom number reaches 72 and keeps low later (figure 6). This also means that the cluster becomes stable from this moment on.

At the beginning of our simulation, we expected to find that the $\overline{R}_{g,p}$ would decrease suddenly at a moment, but we did not know whether the Ti–O cluster's structure would be transformed again as these clusters grew larger and larger after a transformation. We unexpectedly found that the $\overline{R}_{g,p}$ again abruptly decreases when the atom number reaches around 126, and it remains stable at about 1.1 Å thereafter (stage). This indicated that, despite the fact that the cluster had already done it once, there was a transformation from one type of titanium oxide to another when $N = 120$–126 and the size of the cluster was about 8.4 Å × 11.0 Å × 36.0 Å.

To identify the type of a Ti–O cluster after transformation, we compared our structure with the standard crystal structures of TiO [25], $TiO_{2\text{-rutile}}$ [26], $TiO_{2\text{-anatase}}$ [27], Ti_2O_3 [28] and Ti_3O_5 [29] (table 1). We extended these structures in three directions to 21 Å × 36 Å × 40 Å to calculate the $\overline{R}_{g,p}$ value and to perform RDF statistical analysis [30].

Table 1. Parameters for TiO_x crystal structure (from MS database).

Structure	a (Å)	b (Å)	c (Å)	α (°)	γ (°)	β (°)	Space group
TiO	4.293	4.2930	4.2930	90	90	90	*Fm*3*m* (225)
$TiO_{2\text{-rutile}}$	3.8400	3.8040	9.6140	90	90	90	*I*41/*amd* (141)
$TiO_{2\text{-anatase}}$	4.5941	4.5941	2.9589	90	90	90	*P*42/*mnm* (136)
Ti_2O_3	5.1580	5.1580	13.6110	90	90	120	*R*3*ch* (167)
Ti_3O_5	9.7568	3.8008	9.4389	90	91.5	90	*C*12/*m*1 (12)

The calculated $\overline{R}_{g,p}$ values of the extended crystal structure are as follows: 1.2213 Å for TiO, 1.1988 Å for $TiO_{2\text{-rutile}}$, 1.3125 Å for $TiO_{2\text{-anatase}}$, 1.1211 Å for Ti_2O_3, 1.0988 Å for Ti_3O_5. We compared each of these values to those of the simulated Ti–O clusters (figure 4). When the atom number of a simulated cluster is from 72 to 120, its $\overline{R}_{g,p}$ value is close to the calculated value for TiO (1.2213 Å) and for $TiO_{2\text{-rutile}}$ (1.1988 Å). When the atom number is precisely at the formation point of 72, the Ti:O ratio in the simulated Ti–O cluster is close to 1:1. We believe that the titanium oxide formed at this stage is closer to TiO than $TiO_{2\text{-rutile}}$. When the atom number is 126 or greater, the titanium oxide may be closer to the structure of Ti_3O_5 or Ti_2O_3. We depended on the RDF calculation result to determine which.

We calculated RDFs for Ti–O clusters with atom numbers of 126 and 4335, which represent two growth states, the first immediately after transformation and the second after a long period of growth (figure 7). We also calculated RDFs for the standard supercell crystal structures of Ti_2O_3 and Ti_3O_5. The RDFs for our Ti–O clusters with atom numbers of 126 and 4335 have the same number of peaks as the RDF for Ti_3O_5, and the peaks are in similar positions. However, the RDFs in the cluster's curve whose atoms number of 126 show no sharp peak, the signal of long range ordered structure, which means that it is not crystal structure but more like amorphous Ti_3O_5 structure. Since we already knew from the $\overline{R}_{g,p}$ analysis that our clusters after transformation had to be either Ti_2O_3 or Ti_3O_5, this RDF result tipped the scale to amorphous Ti_3O_5 structure. This result is consistent with our previous TEM results showing that the structure of our oxide is Ti_3O_5 [31]. Using XRD, Jong-Oh *et al* identified the equilibrium titanium oxide phase as Ti_3O_5 in Fe alloys when Ti content is less than 2.1% [32].

3.3. Effect of environment on Ti–O clusters

The morphology and structure of Ti–O clusters are affected by the environment in which cluster growth and nucleation occur. We studied the effect of environment on internal compactness ($\overline{R}_{g,p}$) and on the external morphology (degree of sphericity) of simulated clusters. The $\overline{R}_{g,p}$ values for our simulated clusters were a little lower in a molten iron environment, indicating greater internal compactness (table 2). We speculated that this compactness was the result of the pressure of the surrounding molten iron atoms on the Ti–O clusters.

In both environments, molten iron and vacuum, the degree of sphericity of clusters whose atom number was smaller than 25 was between about 0.85 and 1, indicating that their shape corresponded closely to that of the ideal sphere (figure 8). In a vacuum, the degree of sphericity remained between 0.75 and 0.9 even with higher and higher atom numbers, and cluster morphology was nearly spherical in all cases. In the molten iron environment, however, only small clusters were spherical. For those whose atom number was greater than 25, their degree of sphericity was lower for higher atom numbers, reaching as low as 0.4 for a cluster with 350 atoms. Cluster geometry was more diverse with higher atom numbers, stretching into branch or worm-like morphology.

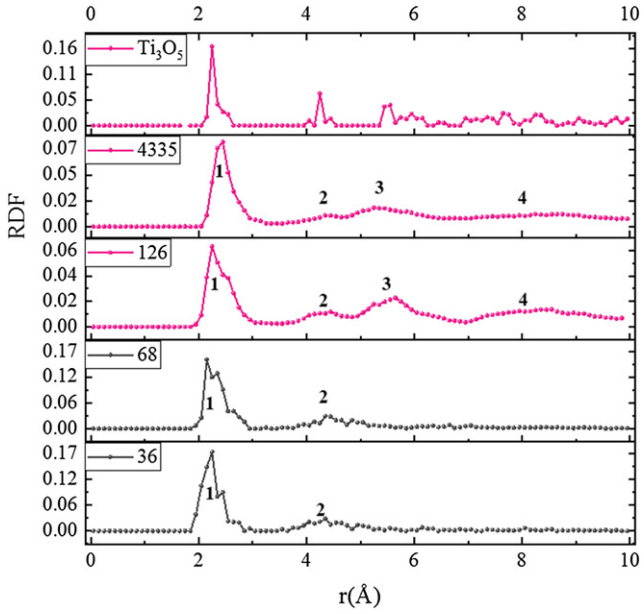

Figure 7. Radial distribution functions of Ti–O. The bottom four curves are the RDF of our simulated clusters. The top curve is the RDF of known crystal structures Ti_3O_5. The RDFs of clusters whose atom numbers are 36 and 68 show two peaks (numbered 1 and 2), indicating that these clusters have short-range ordered structure (long-range disordered). The RDFs of clusters whose atom numbers are 126 and 4335 show four number of peaks, indicating that these clusters have similar structure with the known crystal structure of Ti_3O_5.

Table 2. The $\overline{R}_{g,p}$ values in different environments. All simulated clusters are before formation.

Atom number of simulated clusters	$\overline{R}_{g,p}$ (Å) in a vacuum	$\overline{R}_{g,p}$ (Å) in molten iron
8	1.182	1.180
24	1.454	1.444
30	1.510	1.493
32	1.522	1.502
46	1.565	1.534
68	1.622	1.609

Because the sphere is the shape with the least surface energy, we expected the most stable clusters in our simulation to take that shape, but that was not the case. The worm-like shapes of our mature clusters probably resulted from the effect of their molten iron environment. In our previous study, we extracted a worm-like Ti–O cluster from a molten iron simulation box and inserted it into a vacuum box. Its shape almost immediately curled into a sphere in the new environment [2]. We speculated that the vacuum allowed the cluster to seek the morphology with the lowest possible surface energy. By contrast, clusters in the presence of molten iron

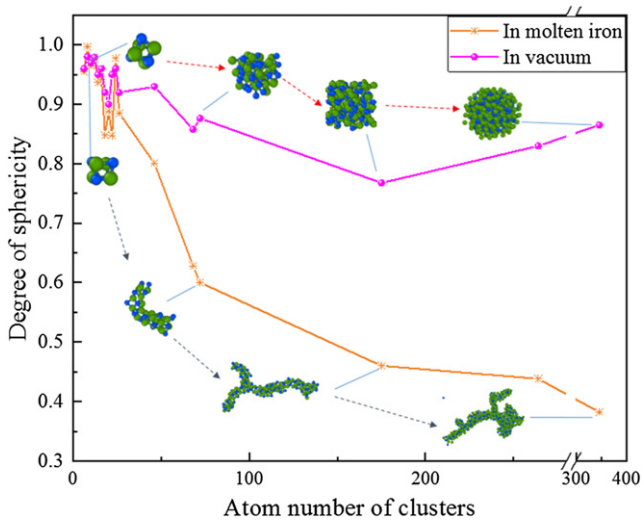

Figure 8. The relationship between degree of sphericity and atom number in clusters.

would be forced to accommodate their shape to the surrounding environment. In our current study, we confirmed that this was the case.

4. Conclusions

Using simulated Ti–O clusters, we described their morphology, identified their critical formation size, and traced their transformations at certain points in growth process. Our conclusions were as follows:

(a) The structure evolution of Ti–O clusters in molten iron had three stages: unstable clusters $\rightarrow$ amorphous TiO structure $\rightarrow$ amorphous Ti_3O_5 structure

(b) The mean critical size for the formation of amorphous TiO structure is about 7.0 Å $\times$ 9.6 Å $\times$ 21.6 Å. The critical size for the transformation of amorphous Ti_3O_5 structure is about 8.4 Å $\times$ 11.0 Å $\times$ 36.0 Å.

(c) The $\overline{R}_{g,p}$ value, which was inversely related to compactness, increased with the growth of clusters until structure transformation occurred, then decreased abruptly. Once the clusters formed a particular type of titanium oxide, the $\overline{R}_{g,p}$ value remained stable until transformation.

(d) Morphology changed as Ti–O clusters grew. Morphology was planar when the atom number was 4 or less, cuboid when the atom number was from 6 to 30, and dendritic when the atom number was from 32 to 68. When the atom number was greater than 72, the dendrites grew branches.

Conflict of interest

We declare that we do not have any commercial or associative interest that represents a conflict of interest in connection with this work.

Acknowledgments

This work was supported by State Key Laboratory of Advanced Special Steel, Shanghai Key Laboratory of Advanced Ferrometallurgy and the Science and Technology Commission of Shanghai Municipality (No. 19DZ2270200). The manuscript was finalized when Dr. Li worked as a visiting scholar at the National High Magnetic Field Laboratory, which is supported by NSF DMR-1644779 and the State of Florida. Thanks to the High-Performance Computing Center of Shanghai University and Shanghai Engineering Research Center of Intelligent Computing System (No. 19DZ2252600) for providing the computing resources and technical support. Thanks also to Mary Tyler for editing.

Data availability statement

All data that support the findings of this study are included within the article (and any supplementary files).

ORCID iDs

Liang He https://orcid.org/0000-0003-0506-1278

References

[1] Mandel' A E *et al* 2003 Light-induced absorption in bismuth titanium oxide crystals illuminated with narrow-band light *Russ. Phys. J.* **46** 1237–44
[2] Yang L, Zhang W, He L, Li H and Zheng S 2019 Study on the growth and morphology evolution of titanium oxide clusters in molten iron with molecular dynamics simulation *RSC Adv.* **9** 32620–7
[3] Bao W, Zhang W, Li H, Zheng S and Zhai Q 2017 A first-principles study of titanium oxide clusters formation and evolution in a steel matrix *RSC Adv.* **7** 52296–303
[4] Gibbs J W 1878 On the equilibrium of heterogeneous substances *Am. J. Sci.* **s3-16** 441–58
[5] Mahata A, Zaeem M A and Baskes M I 2018 Understanding homogeneous nucleation in solidification of aluminum by molecular dynamics simulations *Modelling Simul. Mater. Sci. Eng.* **26** 025007
[6] Radha A V, Forbes T Z, Killian C E, Gillbert P U P A and Navrotsky A 2010 Transformation and crystallization energetics of synthetic and biogenic amorphous calcium carbonate *Proc. Natl Acad. Sci. USA* **107** 16438–43
[7] Fratzl P, Fischer F D, Svoboda J and Aizenberg J 2010 A kinetic model of the transformation of a micropatterned amorphous precursor into a porous single crystal *Acta Biomater.* **6** 1001–5
[8] Verch A, Gebauer D, Antonietti M and Cölfen H 2011 How to control the scaling of $CaCO_3$: a 'fingerprinting technique' to classify additives *Phys. Chem. Chem. Phys.* **13** 16811
[9] Chakraborty D and Patey G N 2013 Evidence that crystal nucleation in aqueous NaCl solution occurs by the two-step mechanism *Chem. Phys. Lett.* **587** 25–9
[10] Faken D and Jónsson H 1994 Systematic analysis of local atomic structure combined with 3D computer graphics *Comput. Mater. Sci.* **2** 279–86
[11] Koradi R, Billeter M and Wüthrich K 1996 MOLMOL: a program for display and analysis of macromolecular structures *J. Mol. Graph.* **14** 51–5
[12] Liu F and Sun D 2019 Ion distribution and hydration structure at solid–liquid interface between NaCl crystal and its solution *ACS Omega* **4** 18692–8
[13] Ding W, Liu G W, Yu T and Qu G M 2010 The molecular dynamics simulation of HEWL in different conditions *Comp. Appl. Chem.* **27** 173–8
[14] Plimpton S 1995 Fast parallel algorithms for short-range molecular dynamics *J. Comput. Phys.* **117** 1–19

[15] Alderman O L G, Skinner L B, Benmore C J and Weber J K R 2014 Structure of molten titanium dioxide *Phys. Rev.* **90** 094204
[16] Svergun D I 1993 A direct indirect method of small-angle scattering data treatment *J. Appl. Crystallogr.* **26** 258–67
[17] Meng F Z 2001 An empirical formula of improvement for calculation of paraffin gyration radius *J. Dezhou Univ.* **17** 53–5
[18] Gmachowski L 2000 Estimation of the dynamic size of fractal aggregates *Colloids Surf.* A **170** 209–16
[19] Robert-Inacio F, Boschet C, Charollais F and Cellier F 2006 Polar studies of the sphericity degree of V/HTR nuclear fuel particles *Mater. Charact.* **56** 266–73
[20] Datta A, Kirca M, Fu Y and Albert C 2011 Surface structure and properties of functionalized nano diamonds: a first-principles study *Nanotechnology* **22** 065706
[21] Lee E-K, Choi H, Lee S-G and Chung Y-C 2010 Energetics of Pb heterostructures formation on the Cu (111) in the early stage of the deposition process *J. Appl. Phys.* **107** 114315
[22] Gotoh K 2012 Radial distribution function *Part. Morphol.* **1** 37–59
[23] Gunton J D 1999 Homogeneous nucleation *J. Stat. Phys.* **95** 903–23
[24] Lundqvist M J, Nilsing M, Persson P and Lunell S 2010 DFT study of bare and dye-sensitized TiO_2 clusters and nanocrystals *Int. J. Quantum Chem.* **106** 3214–34
[25] Yu T H, Lin S J, Chao P, Fang C S and Huang C S 1974 A preliminary study of some new minerals of the platinum-group and another associated new one in platinum-bearing intrusions in a region of China *Acta Geol. Sin.* **2** 202–18
[26] Baur W H and Khan A A 2010 Rutile-type compounds: IV. SiO_2, GeO_2 and a comparison with other rutile-type structures *Acta Crystallogr.* B **27** 2133–9
[27] Horn M, Schwebdtfeger C F and Meagher E P 1972 Refinement of the structure of anatase at several temperatures *Z. Kristallogr.* **136** 273–81
[28] Rice C E and Robinson W R 1977 Structural changes in the solid solution $(Ti_{1-x}V_x)_2O_3$ as x varies from zero to one *J. Solid State Chem.* **21** 145–54
[29] Grey I E, Li C and Madsen I C 1994 Phase equilibria and structural studies on the solid solution $MgTi_2O_5$–Ti_3O_5 *J. Solid State Chem.* **113** 62–73
[30] Wang Y, Shi Y, Zhao C, Zheng Q and Zhao J 2019 Photogenerated carrier dynamics at the anatase/rutile TiO_2 interface *Phys. Rev.* B **99** 165309
[31] Wang T, Bao W Q, Zheng S B, Zhai Q and Li H 2017 A Study on the size and type of inclusions in Si–Mn combined deoxidated low carbon steel strip *TMS2017 Annual Meeting and Exhibition* (San Diego)
[32] Jo J-O, Kim W-Y, Kim D-S and Pak J-J 2008 Thermodynamics of titanium, nitrogen, and oxygen in liquid alloy steels *Met. Mater. Int.* **14** 531–7